

Fabric Preserving and Fabric Destroying Dolomitization: A case of Seawater Dolomitization

Alham Jassim Al-Langawi

Authority of Applied Education and Training, College of Education, Department of Science, Kuwait, Email: alhamaqeel@hotmail.com.

:

:

)

(

()

ABSTRACT: This study is based on field, petrographic and geochemical investigations of Hajar Supergroup autochthonous rocks: Ruus Al Jibal Group- Musandam Peninsula, and Akhdar Group- Jebel Akhdar, Oman and U.A.E., and para-autochthonous Maqam Formation-Sumeini Group-Jebel Sumeini-U.A.E. Petrographic evidence indicates that the rocks were deposited in a shallow marine shelf environment, particularly tidal flat, lagoon, reef, back-reef and shoal environments that were part of the Arabian Platform during Permian and Triassic times. However, they are almost entirely dolomitized and the rocks show different petrographic features ranging from perfect preservation of original texture by mimetic dolomitization to complete obliteration and destruction of the original limestones giving rise to inequicrystalline and equicrystalline fabrics. Dolomites analyzed by geochemical methods were categorized on the basis of textural variations; crystal size, shape and impurity or inclusion distribution within crystals, and whether these crystals are found as rock forming (replacive) or cements. The dolomites display variations in stoichiometry, ordering and trace element concentrations indicating differences in dolomitizing fluid chemistry and recrystallization stages that prevailed through time. It indicates also that although dolomitization is pervasive, dolomites are petrographically and chemically immature. All the petrographic and geochemical evidence strongly indicates seawater and/or mixing zone dolomitization which may have been initiated soon after deposition of the host sediments. Rocks showing preservation of allochems as well as the marine cements by mimetic dolomite crystals, suggest that dolomitization was early (at shallow depths) with very active marine-water circulation and occurred in a relatively short time. Evidence from crystalline dolomites indicates several crystallization events at shallow burial depths, under marine waters modified by increased temperature and mixing probably with evaporitic brines. The only fluid capable of early dolomitization in the case of the Oman Mountains dolomites was warm seawater from the Tethys Ocean which was circulating in the subsurface.

KEYWORDS: Fabric preserving dolomitization, fabric destroying dolomitization, permian and triassic rocks, Oman mountains, seawater dolomitization.

1. Introduction

The Permian and Triassic rocks studied here include dolomites which were sampled from: Wadi Al Bih and Wadi Hajil-Musandam Peninsula, Jebel Sumeini, Wadi Bani Kharus, Wadi Hajir and Wadi Bani Harras-Jebel Akhdar (Figure 1 and 2). Dolomites are described according to grain size, crystal shape, presence or absence of inclusions and their distribution within the crystals, and degree of preservation of the depositional texture. Dolomites are divided into those which show good preservation of the depositional fabric of the original limestone (fabric-preserving or mimetic dolomitization) and those where there is little or no evidence of the original limestone fabrics (fabric-destroying dolomitization). In the latter case crystal textures are described using the terminology of Sibley and Gregg (1987). The rocks that underwent fabric-destroying dolomitization show equicrystalline and inequicrystalline textures which are planar (idiotopic), nonplanar (xenotopic), and hypidiotopic, with crystals showing differences in impurity distribution.

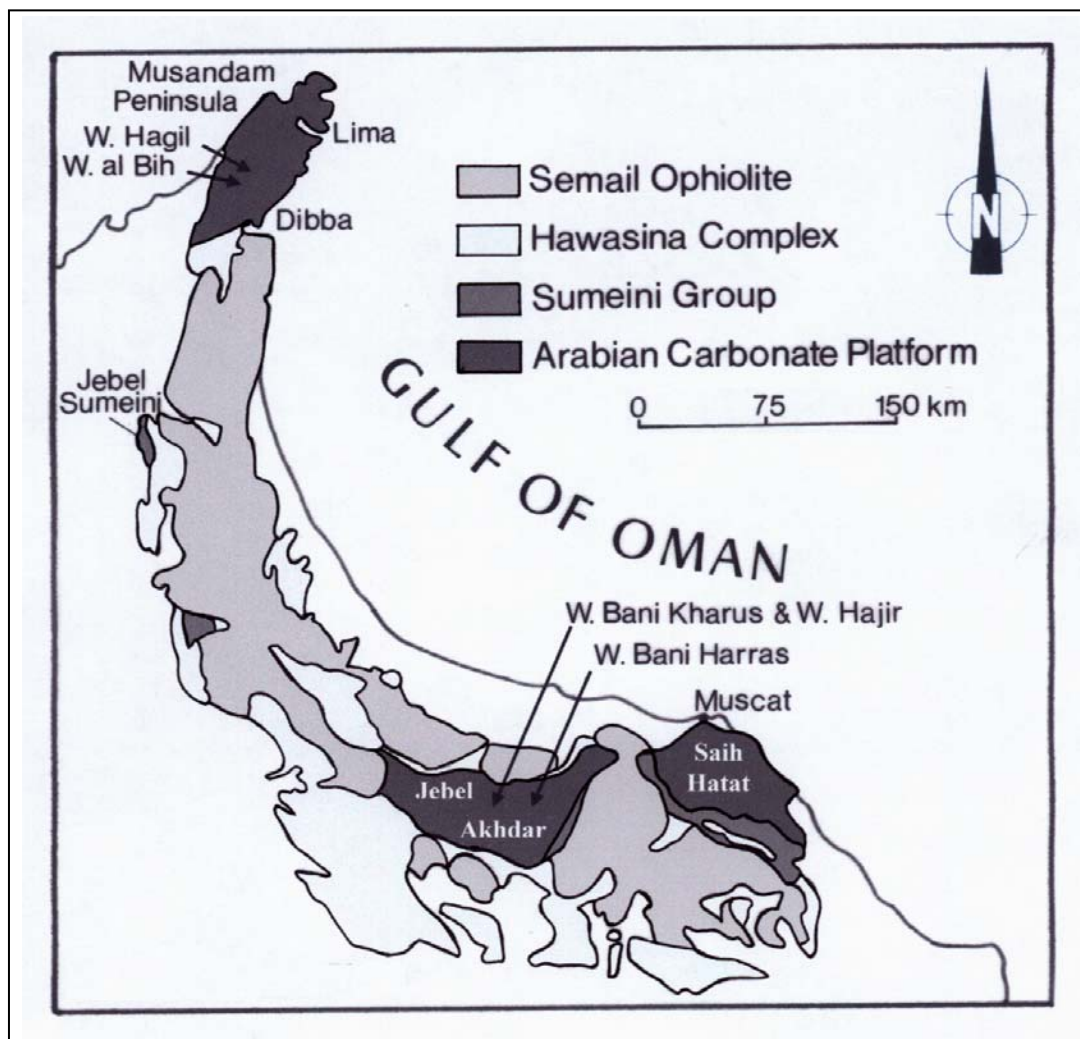


Figure 1. A map showing simplified geology of the Oman Mountains and major fieldwork localities.

2. Methods used for petrographic and chemical investigation.

The petrographic investigations were carried out by using transmission light microscope, scanning electron microscope, and cathodoluminescence. After the petrographic investigation of all samples (220 samples were examined petrographically using thin sections) dolomites were categorised on the basis of textural variations; crystal size, shape and impurity or inclusion distribution within crystals, and whether occurring as rock forming (replacive) or as cements. The Color Illustrated Guide to Carbonate Rock Constituents (Scholle, 1978) and the Atlas of Sedimentary Rocks Under the Microscope (Adams *et al.*, 1984) were used as aids in determining the appropriate name for the dolomites exhibiting preserved host-limestone textures. In order to get an indication of the nature of the original limestone texture and structure in samples with little obvious fabric preservation a sheet of white paper was inserted between the thin section and the stage and the light intensity increased. This

technique is referred to as the “white paper technique”, also known as white card technique (Delgado, 1977; Zenger, 1979).

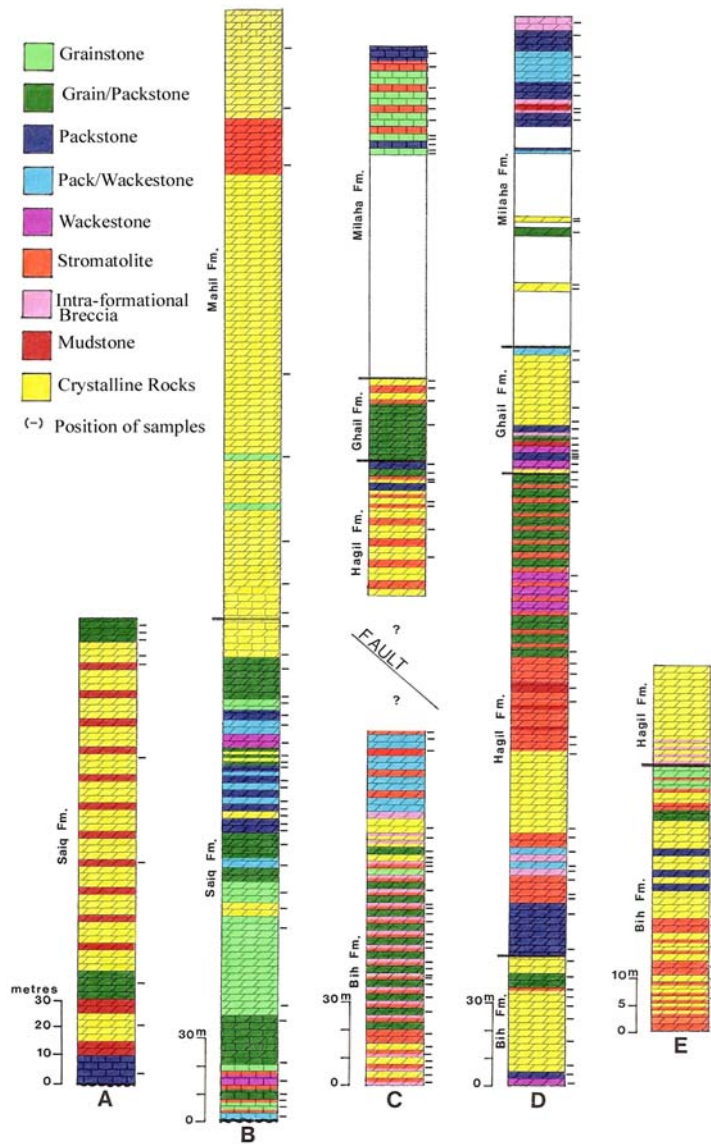


Figure 2. Stratigraphic columns of the Ruus Al Jibal and Akhdar Groups, and Milaha Formation From all studied locations. A) Wadi Bani Harras, B) Wadi Bani Kharus, C) Wadi al Bih (locations 1-8), D) Wadi al Bih (location 9), E) Wadi Hagil.

Cathodoluminescence photomicrographs are used to show the differences in dolomite and calcite trace element composition and to determine the cross-cutting relationship between the different fabric components in the samples. The description of colours was based on what was observed while examining the polished thins under the beam. Although the beam voltage and current were kept constant, the quality and intensity of colours

FABRIC PRESERVING AND FABRIC DESTROYING DOLOMITIZATION

in the photomicrographs are different. This was due to either the quality of film used in the photography, or to the exposure times used to enhance differences.

The petrographic investigations were supplemented by geochemical analysis, using microprobe, X-ray diffraction, ion chromatography, atomic absorption, stable isotopes, and quantitative analysis by the scanning electron microscope.

3. Dolomite textures and fabrics.

3.1 Fabric-preserving dolomitization

The terms “fabric-preserving” or “mimetic dolomitization” are given to rocks showing selective replacement of original limestones by dolomite crystals without any destruction of the original relationships between the fabric components (Sibley, 1980; Sibley, 1982; Bullen and Sibley, 1984; Sibley, 1990; Purser *et al.*, 1994a and b). The fabric-preserving texture in dolomites is controlled mainly by two major factors; the precursor mineralogy and grain/crystal size (Murray and Lucia, 1967; Sibley, 1982; 1990). The previous authors suggested that high magnesium calcite tends to be dolomitized with retention of the primary fabrics, whereas low magnesium calcite is more resistant to dolomitization and replacement results in fabric-destroying textures. Tucker and Wright (1990) explained the retention of the host limestone fabrics after dolomitization as being a result of the balance between dissolution and dolomite precipitation.

The fabric-preserving dolomites studied here exhibit grain-supported and mud-supported textures that can be classified into; stromatolitic dolomites, intraformational breccias, dolomudstones, wackestones, packstones, and grainstones. The wackestones, packstones and grainstones are mainly bioclastic, oolitic and pisolitic. The preserved depositional features suggest that these rocks were deposited in shallow subtidal, intertidal and supratidal environments with variable wave energy levels. Two main fabric components can be distinguished in the rocks which underwent fabric-preserving dolomitization. These are microcrystalline dolomite and void filling dolomites.

3.1.1 Microcrystalline rock-forming dolomites

The rock forming microcrystalline dolomite crystals are generally $\leq 8 \mu\text{m}$ in size. These crystals either replaced the original allochems or matrix in granular host limestones, or the carbonate mud of stromatolites and mudstones. The microcrystalline dolomites tend to be cloudy and anhedral giving rise to very fine nonplanar textures (Figure 3). At some stratigraphic levels the microcrystalline dolomites which replaced pellets and geopetal sediments within fenestrae were affected by aggrading neomorphism, which resulted in the production of larger sizes and the development of some planar boundaries. These aggraded crystals often show the same luminescence as void filling dolomite crystals in the same samples. Microcrystalline dolomites also replaced micrite envelopes and wall structure of some bioclasts, such as forams and algal grains (Figure 3). This replacement helped in preserving parts of the fabric components as relicts even at later stages of pervasive dolomitization which resulted in the development of crystalline texture. Cathodoluminescence of rocks exhibiting fabric-preserving textures showed that all the microcrystalline dolomites have homogeneous dull brownish-red to orange-red luminescence, or with dark-grey luminescence (Figure 4). Some original oolitic grainstones and packstones show good textural and structural preservation of the rock components.

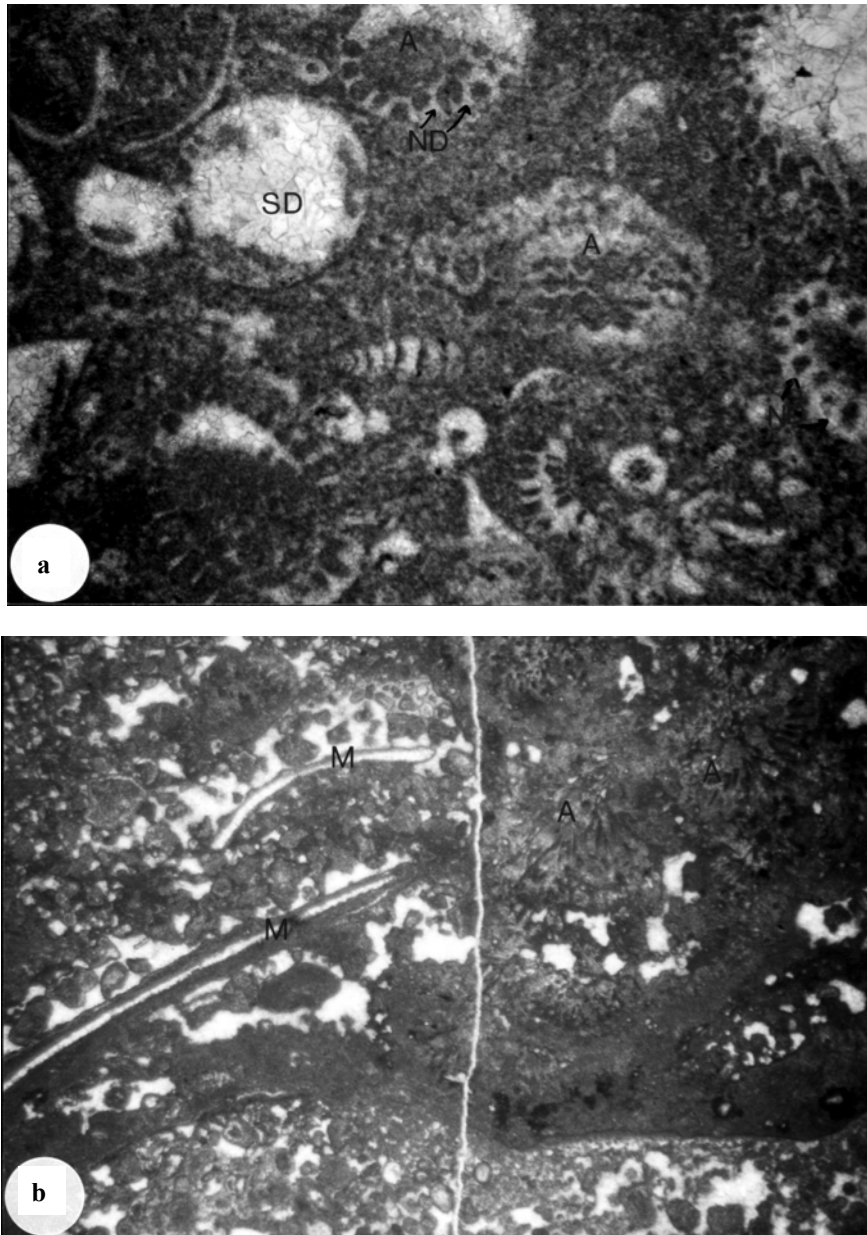


Figure 3. Photomicrographs taken with plane polarized light of: (a) dolomite with mud-supported textures from the Saiq Formation, Kharus15; the internal structure of the algal fragments [A], and the matrix are replaced by microcrystalline cloudy dolomite and the intragranular, mouldic and fracture porosities are filled by planar sparry dolomite mosaics [SD] and nonplanar fine dolomite cement [ND]. (b) a peloidal-biocalcific packstone which is composed of molluscan [M] and algal fragments [A], from Hagil Formation, Bih31. (c) a biocalcific wackestone, the biocalcifics are algal [A] remains and ostracods shells [O], this rock show the replacement of original carbonate mud by microcrystalline dolomite, and the filling of the fenestral, mouldic, intergranular and fracture porosity by clear dolomite mosaics. Field of view= 8.75 mm.

FABRIC PRESERVING AND FABRIC DESTROYING DOLOMITIZATION

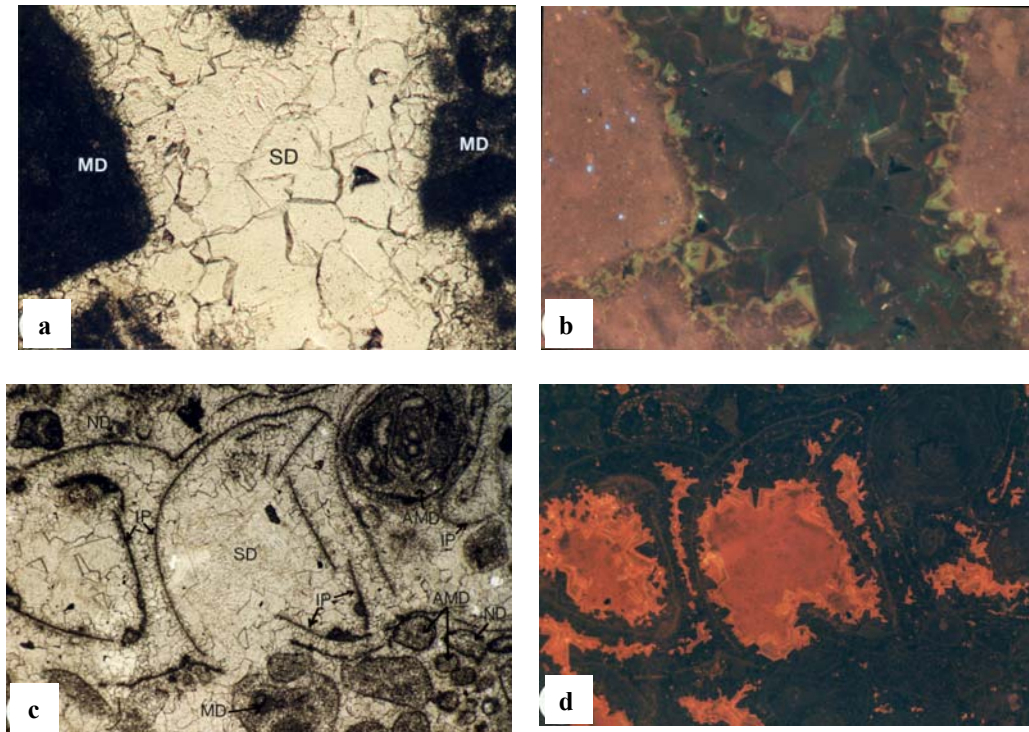


Figure 4. (a) A photomicrograph taken with plane polarized light of a part of an intraformational breccia where all the clasts are replaced by microcrystalline dolomite [MD] and the intergranular pore spaces are filled by clear drusy dolomite mosaics [SD]. (b) Cathodoluminescence photomicrograph showing the same view as in (a); the microcrystalline and very fine nonplanar dolomites produce brownish-red luminescence, whereas the sparry dolomites start as dark brownish-red and then share a light green luminescent zone. The coarser sparry dolomites are faintly zoned displaying dark brownish red and dark green luminescence. Bih Formation-WBB31, field of view = 1 mm. (c) A photomicrograph taken with plane polarized light of a bioclastic peloidal grainstone; the original carbonate mud is replaced by microcrystalline dolomite [MD], some of which are aggraded into dolomite microsars [AMD]. Intra-granular and mouldic pore spaces are filled by very fine clear nonplanar dolomite [ND]. The rock was affected by isopachous cement now replaced or may be precipitated directly as dolomite? [IP], and later cementation by planar sparry dolomite mosaics [SD]. Compaction resulted in grain fracturing occurred after the isopachous cementation. (d) Cathodoluminescence photomicrograph of (c) showing the following luminescence for each fabric component; brownish-red for the microcrystalline dolomite and isopachous dolomite crystals, the very fine nonplanar and the fine subhedral dolomite cement are nonluminescent, the medium subhedral sparry dolomites show alternating red and orange zonation and homogeneous red, and the coarse sparry dolomite show homogeneous red luminescence. Saiq Formation-Kharus7, field of view= 2.5 mm.

The ooids are formed of alternating concentric layers of microcrystalline dolomites and slightly coarser, nonplanar cloudy and clear dolomite crystals. It is not certain whether these different structural preservation modes reflects variations in ooid composition, or is due to predolomitization diagenesis and fluctuations in dolomitizing environments from marine to meteoric or mixed water conditions. The cathodoluminescence patterns of the microcrystalline, and cloudy very fine and fine nonplanar dolomite crystals within ooids are always comparable to the luminescence in other replacive microcrystalline dolomites, whereas the luminescence

of the clear fine nonplanar or planar dolomite crystals within the ooids is comparable to the luminescence of void filling sparry dolomite crystals (Figure 5). These variations in the luminescent patterns and interrelationships between the fabrics indicate that all the microcrystalline and very fine-fine nonplanar cloudy dolomite crystals formed under the same fluid conditions which predate dissolution and compaction features in the rocks. The slightly coarser planar clear dolomite crystals formed after meteoric water diagenesis which induced dissolution of the aragonite and/or high Mg-calcite, and after compaction which resulted in grain fracturing.

3.1.2 Void filling dolomites

Void filling dolomites are the crystals found infilling the intergranular, intragranular, fenestral, and fracture porosity within rocks that underwent fabric-preserving dolomitization. They are divided into; isopachous cements and void filling sparry mosaics.

Isopachous cement

Most of the granular dolomites were subjected to early cementation giving rise to isopachous rims around the outer surfaces of allochems. Some samples show evidence for phreatic meteoric water diagenesis, which produced isopachous cement around both the outer surface of allochems as well as the inner boundaries of the mouldic cavities of bioclasts. This indicates a dissolution stage by meteoric-water and probably cementation by isopachous calcite prior to dolomitization. Whether the isopachous dolomite is of replacement or cement origin is of great importance to this study. Staining with Alizarin Red-S and backscattered images revealed that the isopachous crystals are composed of dolomite.

The isopachous crystals are mainly prismatic, and to a lesser extent rhombic, and are generally $\leq 20 \mu\text{m}$ long. The prismatic isopachous dolomites are cloudy and clear, while the rhombic isopachous dolomite crystals are clear or show alternating clear and cloudy zones. Cathodoluminescence study indicates that the cloudy prismatic isopachous and the cores of rhombic isopachous dolomites in some samples, develop under the same conditions as the microcrystalline dolomites which replaced the allochems and micrite envelopes (Figs. 4 and 5). The clear isopachous prismatic dolomite crystals show dark-brown and dark-grey luminescence, and black nonluminescence that, in some samples, are capped by thin yellow, orange-red and light green luminescent zones. Cathodoluminescence indicates that the rhombic isopachous dolomite crystals are strongly zoned (Figure 5).

Void filling sparry mosaics

The sparry dolomites mainly have a planar texture, composed of subhedral and euhedral rhombic crystals, which are either clear or cloudy, or have cloudy centres and clear rims. In some sparry dolomites impurities are arranged in zones in any given crystal producing alternating clear and cloudy zones. Backscattered images reveal that some of the cloudy cores of sparry dolomites have calcite inclusions, and that most of the void filling dolomite crystals are lined with minute intracrystalline void spaces. Equant euhedral mosaics are present, especially within the intergranular pore spaces of intraformational breccias and some biomouldic porosity (Figure 3). The crystals comprising the equant euhedral mosaics are nonplanar, cloudy and are always fine-crystalline.

FABRIC PRESERVING AND FABRIC DESTROYING DOLOMITIZATION

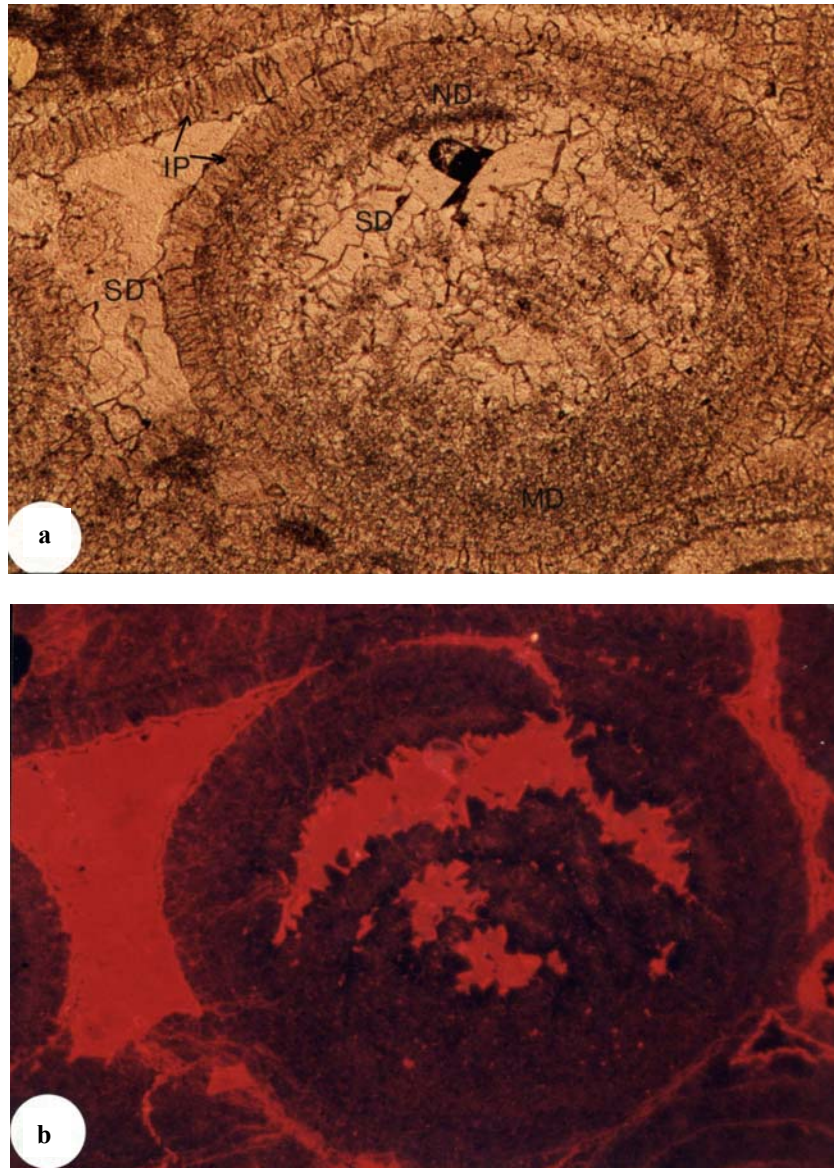


Figure 5. (a) A photomicrograph taken with plane polarized light and (b) Cathodoluminescence photomicrograph of a part of an oolitic grainstone; the microcrystalline dolomite [MD], very fine nonplanar cloudy dolomite spars [ND], and the isopachous dolomite crystals [IP] display dark-grey luminescence. The cloudy isopachous dolomite crystals are capped by a clear rim showing red luminescence and dark-grey terminations (arrow). The clear rhombic [RSD] and subhedral [SD] void filling dolomite crystals display homogeneous red luminescence. The rock was affected by compaction which post dated the precipitation of the isopachous cement and resulted in fracturing the ooids and the cement rim, top centre of the photomicrographs. Saiq Formation-WHS17, field of view = 1 mm.

Investigations with the polarizing microscope and the white paper technique reveal that the void filling sparry dolomites are zoned, especially the medium and coarse crystalline dolomites. Crystals with alternating clear and cloudy zones as seen under transmitted light, produce bright orange-red and yellow luminescence colours at locations with manganese oxides inclusion, and black nonluminescence at places where iron oxide inclusions exist (Figure 5). Calcite inclusions within some dolomite crystals produce speckled orange patterns under cathodoluminescence.

A few samples experienced cementation by coarse sparry dolomite crystals exhibiting curved crystal boundaries, curved cleavages, and sweeping extinction indicative of saddle dolomite. Clear baroque (saddle) dolomite crystals show homogeneous black nonluminescence patterns, and cloudy crystals and cloudy parts of crystals show speckled patterns of black nonluminescent backgrounds with bright red spots. The latter indicate a replacive origin for baroque dolomite.

3.2 Fabric-destroying dolomitization.

Rocks displaying fabric-destroying dolomitization are crystalline dolomites which exhibit a wide range of shapes and sizes. The crystals comprising these rocks are referred to here as rock forming dolomites. Petrographic studies show the distribution pattern of inclusions, and that most of the rocks lack any relicts. A few coiled forams and echinoderms are the only relicts found. The use of white paper gave better images of the original host limestone texture and structure, although these rocks are pervasively dolomitized (Figure 6). In most crystalline dolomites, especially the ones with wide range of impurity distribution, it is the cloudier crystals that replaced the original allochems, while clearer crystals replaced or filled the intergranular and intragranular porosities of the host rocks. The dolomites that replaced the cement or filled the porosity of the precursor rocks always display planar boundaries, and are clear and coarsely crystalline, whereas rock forming crystals which replaced the original allochems are mainly nonplanar, and are cloudy and fine crystalline. The white paper technique revealed that all fracture and void filling sparry dolomites are clear and have a planar texture, and that boundaries of most of the rock forming dolomites are lined with organic matter or iron oxides.

Backscattered images revealed no calcite inclusions within the rock-forming dolomites. This may indicate that the impurities are minute fluid inclusions which developed during the growth of the dolomite crystals. Clear and cloudy parts of the rock-forming dolomites show different luminescent patterns (Figure 7). Clear rock-forming crystals and clear crystal rims show luminescence identical to the void filling dolomite in the same samples (Figure 7). Dolomite crystals filling intercrystalline pores, vugs, and fractures are mainly zoned, producing patterns composed of alternating thick zones and thin sub-zones of bright red, dull red, yellow and green luminescence, and black nonluminescence.

4. Mineralogical and chemical composition of the dolomites.

4.1 Stoichiometry and ordering.

The samples analysed by X-ray diffraction are of two types; either whole rock samples or separate baroque and normal dolomites. The microcrystalline and fine-crystalline dolomite samples and stromatolitic dolomites show either the lowest degree of ordering (0.43), or poor stoichiometry (53.9 Mole% CaCO_3) (Table 1, and Figure 8).

FABRIC PRESERVING AND FABRIC DESTROYING DOLOMITIZATION

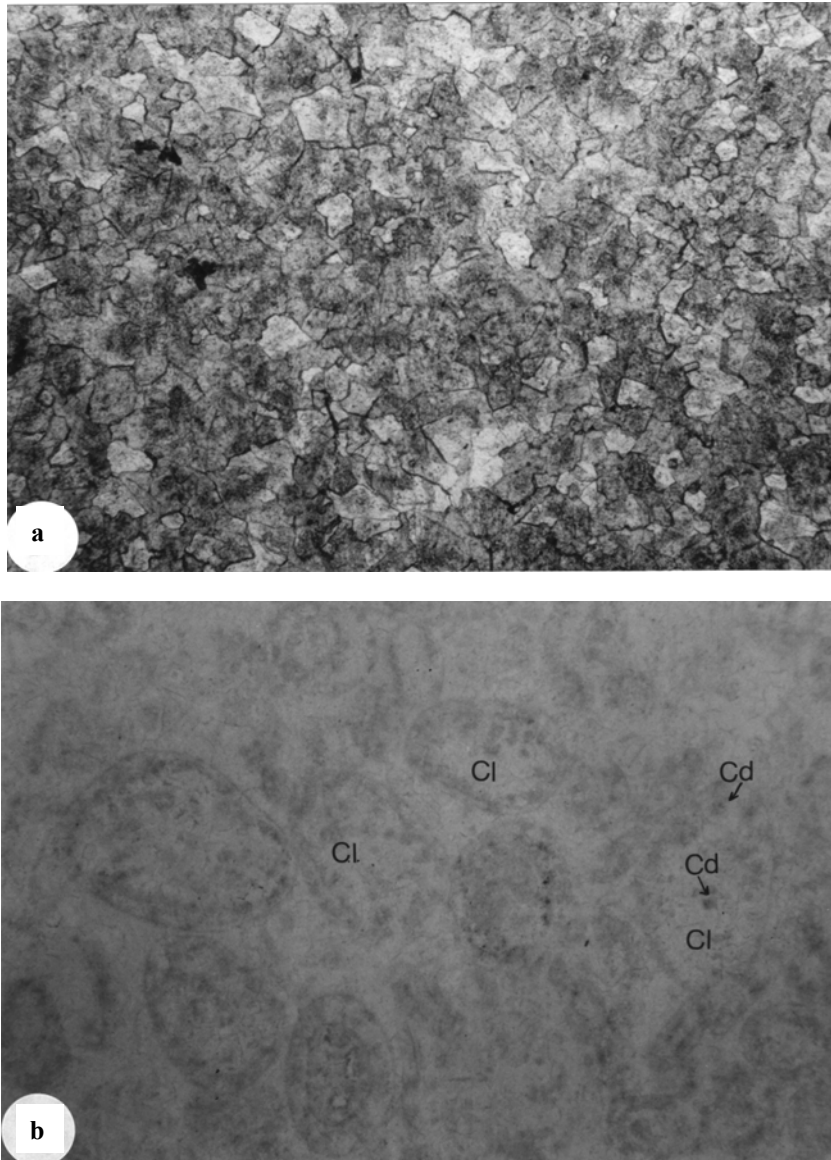


Figure 6. (a) A photograph taken with plane polarized light, (b) the same view but with a sheet of white paper inserted between the thin section and the stage. Although the rock is completely crystalline with no textural preservation of the host rock, there exists a ghost texture of a granular host. The host rock may have been a peloidal and/or oolitic bioclastic grainstone or packstone. The allochems show the effect of meteoric water dissolution which produced intragranular and mouldic porosity that were later cemented by clear crystals [CI] or with crystals having cloudy centres and clear rims [Cd]. The micritic parts are replaced by cloudy dolomite crystals and palaeo-voids are filled by clear dolomite crystals. Bih Formation-Hagil10, field of view = 3.5 mm.

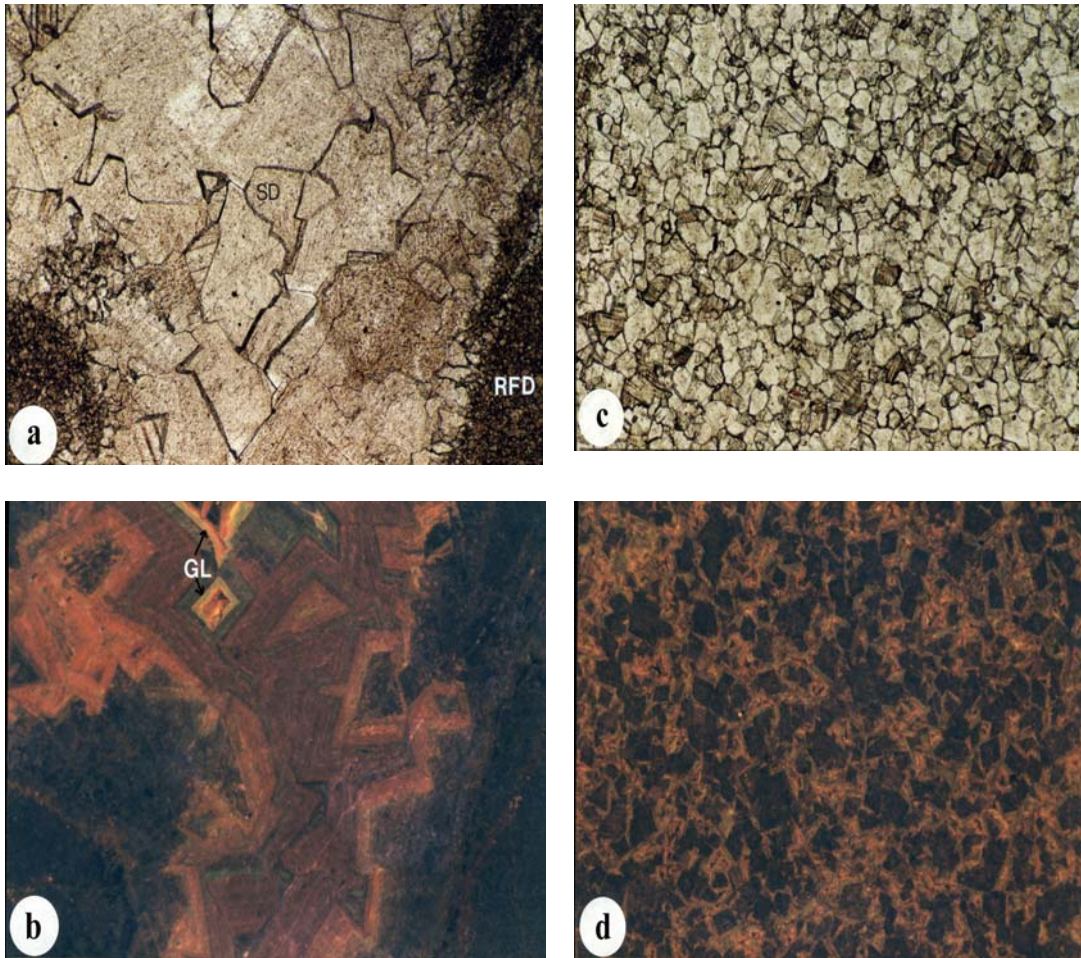


Figure 7. (a) A photomicrograph taken with plane polarized light of a fine crystalline dolomite which is composed of cloudy nonplanar rock-forming crystals [RFD], and cemented by planar sparry dolomite mosaics that reach up to 3 mm in crystals size [SD]. The inclusions within the sparry dolomite crystals decrease towards the centre of the cavities. (b) Cathodoluminescence photomicrograph of (a) showing that the rock-forming dolomite and fine to medium sparry dolomite crystals display brownish-red luminescence. The coarse to very coarse sparry dolomite crystals display alternating red, orange, and brownish-red luminescence, and a thin green-luminescent zone [GL]. Maqam Formation-Member B (SMB10). (c) A photomicrograph taken with plane polarized light of a crystalline dolomite composed of fine to medium rock-forming crystals which are cloudy, clear and with cloudy rhombic centres and clear rims. (d) Cathodoluminescence photomicrograph of (c) showing the cloudy cores and cloudy crystals that display dark brownish-red luminescence, whereas the clear crystals and clear rims display orange luminescence. Maqam Formation Member B (SMB3), field of view = 2.5 mm.

FABRIC PRESERVING AND FABRIC DESTROYING DOLOMITIZATION

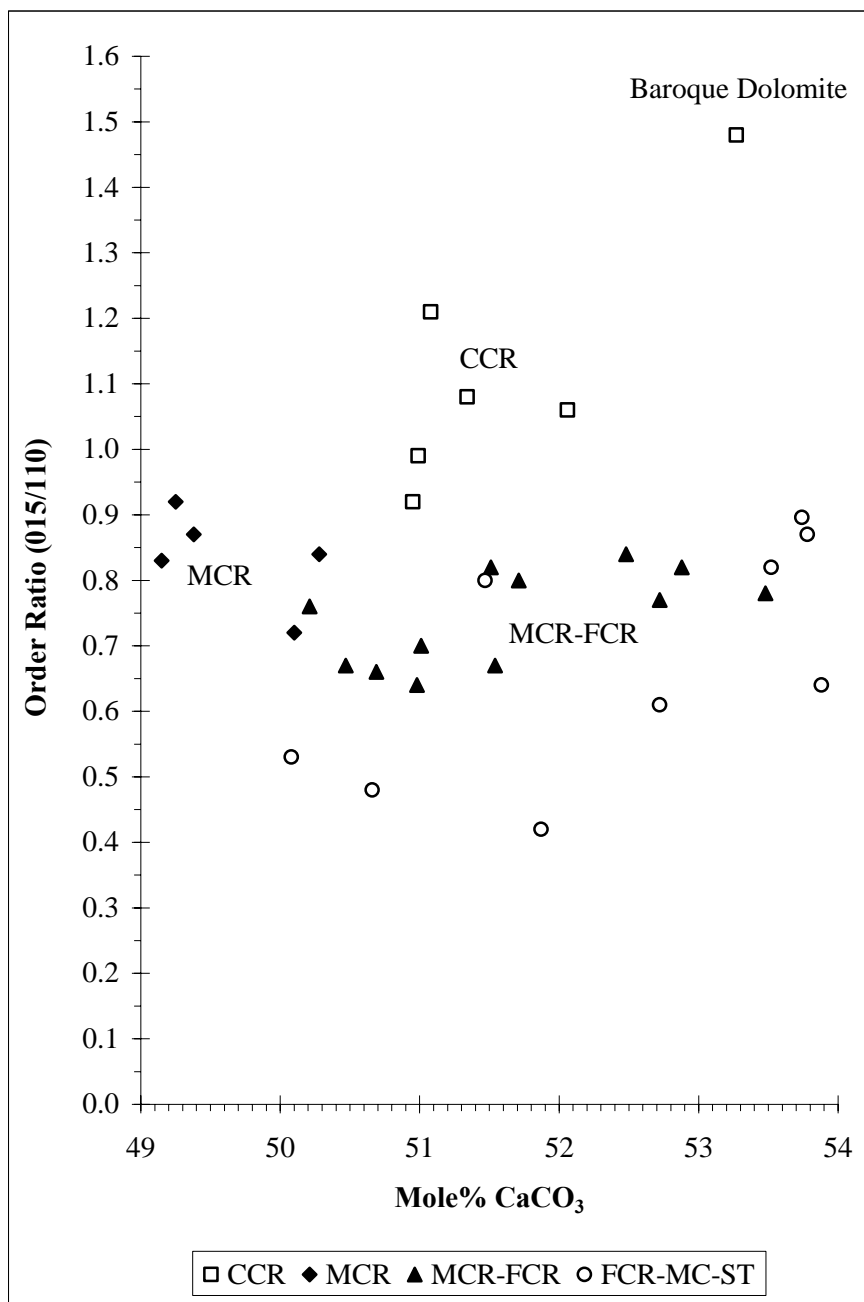


Figure 8. Distribution of different dolomite types according to the degree of ordering and stoichiometry. CCR= Coarse Crystalline, MCR= Medium Crystalline, MCR-FCR= Medium-Fine Crystalline, FCR= Fine Crystalline, FCR-MC-ST= Fine, Microcrystalline, and Stromatolitic.

Inequicrystalline rocks showing crystal size ranging from fine to medium display a wide range of stoichiometry (50-53.5 Mole% CaCO_3) and are poorly to moderately ordered (0.6-0.84). As the dolomite crystals progress into coarser sizes they tend to become more ordered. The medium crystalline dolomites have good stoichiometry (49.2-50.3 Mole% CaCO_3) although intermediate between fine and coarse crystalline dolomite samples in respect to ordering. The baroque dolomite samples show the best ordering, but are nonstoichiometric (53.3 Mole% CaCO_3).

The data collected on Ca and Mg show near-stoichiometric composition for dolomites displaying medium crystalline textures and that most of the microcrystalline, fine and coarse crystalline dolomites are nonstoichiometric (Table 1). Dolomites comprising the rocks which underwent fabric-preserving dolomitization are mainly poorly stoichiometric, and most of the dolomite crystals are Ca-rich. Dolomites comprising the rocks which underwent fabric destroying dolomitization are mainly near stoichiometric (Table 1).

4.2 Trace-element concentration.

Whole rock analysis provided important results, especially for the distribution of Si, Al and SO_4 in the dolomites (Table 2). Rocks which are of stromatolitic and peloidal origin and crystalline rocks that are composed of cloudy rock-forming dolomites display high Al and Si values (1800 and 2304 ppm respectively). The lowest Al and Si values are found in rocks that underwent fabric-destroying dolomitization and which are composed mainly of clear dolomite crystals or crystals with cloudy centres and clear or less cloudy rims (Tables 1 and 2). The SO_4 values, and the Na and Cl values from Table 2, reflect the actual concentrations in the dolomite lattice. The concentration of SO_4 in the samples ranges up to 630 ppm, and tends to be concentrated more in rocks that are of stromatolitic and mudstone origin.

Plotting $\delta^{18}\text{O}$ values against Fe and Mn ppm concentrations for the same samples indicates a general antipathetic relationship between ^{18}O depletion and Mn concentrations, and direct relationship between ^{18}O depletion and the decrease in Fe concentration (Figure 9). Figure 9a shows that as crystal size increases Fe concentrations decrease and crystals tend to become more depleted in ^{18}O . Variations in Fe and Mn concentrations were also evident when the thin sections were examined by cathodoluminescence. The different colour zones were analysed by the microprobe to gain the actual Fe and Mn concentrations. This showed that crystals and zones displaying dark-grey luminescence are relatively Fe-rich (60-9460 ppm) and Mn-poor (0-540 ppm), the crystals and zones that are nonluminescent have Fe and Mn values which are below the detection limits, and that all other luminescent patterns are generally relatively Mn-rich (10-6510 ppm) and with Fe concentrations which are mainly below the detection limit ranges up to 930 ppm). Table 2 shows that Na and Cl tend to be low in the dolomites regardless of texture and composition. Na mean values range from 42-358 ppm, and Cl mean values range from 76-379 ppm. Mn in the whole rock samples is very low, ranging from 10-133 ppm. Excess Na and Cl were plotted against oxygen isotope values (Figure 10b), with the following results: (i) Excluding sample BIH50 (354 ppm excess Na), all the microcrystalline dolomite samples show a general decrease in Cl values and increase in Na concentrations with ^{18}O depletion. Therefore, as the temperature of dolomitizing waters increases (i.e. more depletion in ^{18}O) Na increases and Cl decreases. This suggests that the microcrystalline dolomites with higher Cl concentrations would have formed from initially marine fluids, but as these waters became modified by increasing in temperature (and evaporation?) the crystals became enriched in Na. (ii) Na and Cl concentrations is variable in fine to medium dolomite crystals. Three samples show a general decrease in Cl and increase in Na which is equivalent to what is recognized in the microcrystalline dolomites. (iii) Coarse to very coarse crystalline dolomites become more depleted in ^{18}O they become enriched in Na.

FABRIC PRESERVING AND FABRIC DESTROYING DOLOMITIZATION

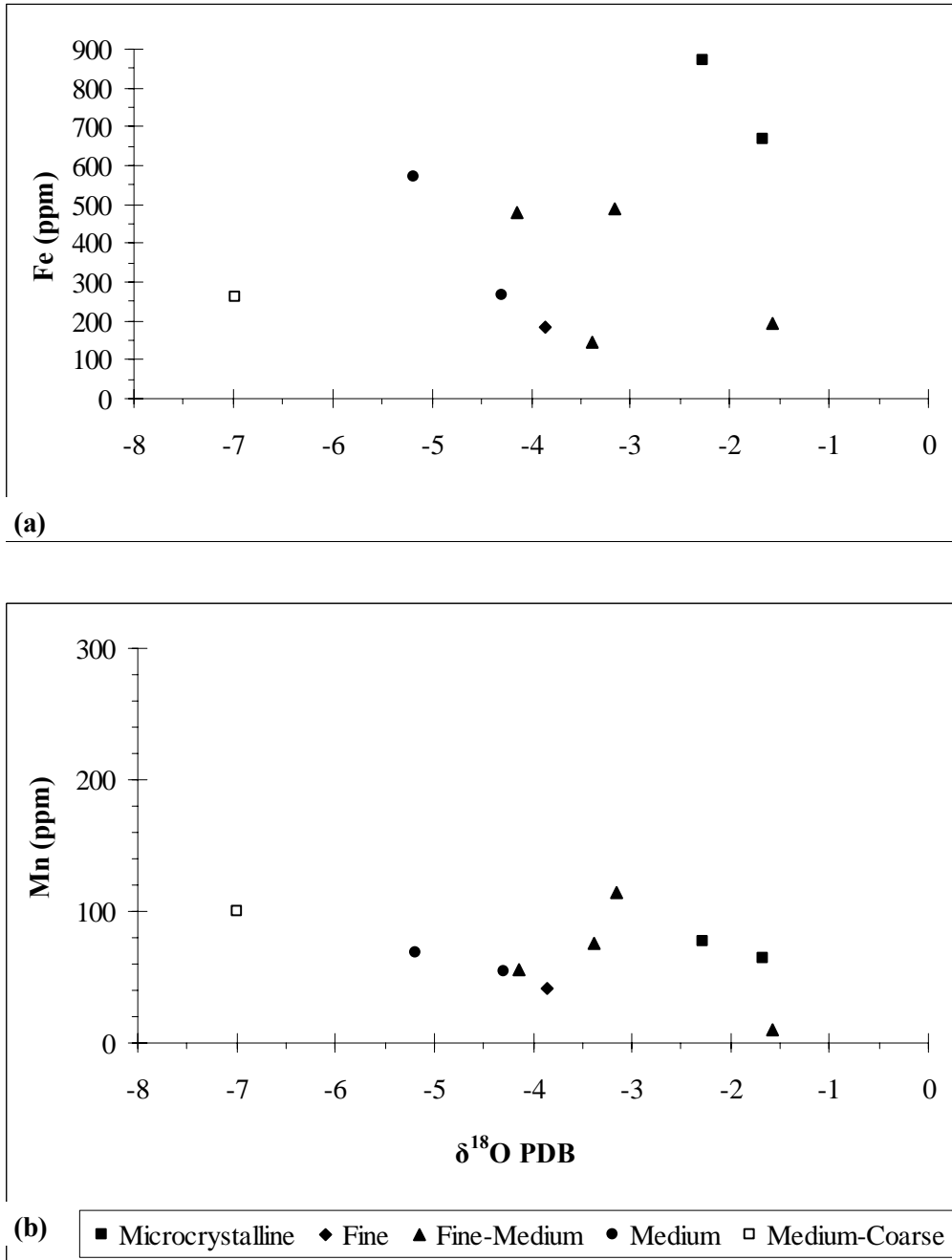


Figure 9. Relationship between crystal size and Mn, Fe and oxygen isotopes concentrations in dolomites.

ALHAM JASSIM AL-LANGAWI

The $\delta^{18}\text{O}$ values for these crystals (-5.954 to -6.987 ‰ PDB) suggest a higher temperature of formation which may be related to an increase in burial or in geothermal gradient. 4) Baroque dolomite sample (BIH29-2) is Na-poor in contrast to all other dolomite samples.

Table 1. Showing degree of ordering and stoichiometry in the dolomites. CCR = Coarse crystalline, MCR= Medium crystalline, FCR= Fine crystalline, MC= Very fine (micritic), ST= Micritic of stromatolitic origin. FP= Fabric Preserving Dolomitization, FD= Fabric Destroying Dolomitization.

No.	Sample No.	Texture (FP), (FD)	Crystal Size	Intensity of Peaks		Degree Of Ordering	Mole % CaCO_3
				[015]	[110]		
1	BIH6	FD	MCR-FCR	169.0	210.3	0.80	51.7
2	BIH10	FD	FCR	148.8	182.3	0.82	53.5
3	BIH29-1	FP	MC	62.4	71.6	0.87	53.8
4	BIH29-2	BAROQUE	CCR	127.7	86.5	1.48	53.3
5	BIH33	FP	FCR-ST	153.8	171.6	0.90	53.7
6	BIH37	FD	MCR-FCR	92.6	122.3	0.76	50.2
7	BIH45	FD	CCR-FCR	171.6	141.6	1.21	51.1
8	BIH46	FD	CCR	163.8	151.3	1.08	51.3
9	BIH50	FP	MC	132.3	207.4	0.64	53.9
10	BIH54	FD	FCR	151.3	185.0	0.82	52.9
11	WBB5	FD	MCR	104.2	144.0	0.72	50.1
12	WBB14	FP	FCR-ST	49.9	104.2	0.48	50.7
13	WBH3	FD	FCR	105.2	200.2	0.53	50.1
14	WBG2	FP	FCR-ST	72.8	173.5	0.42	51.9
15	HAGIL1	FD	MCR-FCR	179.6	231.0	0.78	53.5
16	HAGIL2	FD	MCR-FCR	156.3	190.4	0.82	51.7
17	HAGIL3	FD	CCR-MCR	228.0	216.1	1.06	52.1
18	HAGIL8	FD	FCR-ST	148.8	243.4	0.61	52.7
19	HAGIL16	FD	MCR	204.5	243.4	0.84	50.3
20	HAGIL19	FD	FCR	185.0	231.0	0.80	51.5
21	HAGIL22	FD	MCR-FCR	163.8	213.2	0.77	52.7
22	HARRAS2	FD	MCR	198.8	216.1	0.92	49.3
23	HARRAS4	FD	MCR-FCR	179.6	182.3	0.99	51.0
24	HARRAS5	FD	MCR	144.0	174.2	0.83	49.2
25	HARRAS6	FD	MCR	127.7	146.4	0.87	49.4
26	HARRAS7	FD	MCR-FCR	190.4	228.0	0.84	52.5
27	KHARUS18	FP	MCR-FCR	146.4	228.0	0.64	51.0
28	WHS9	FD	FCR	169.2	254.3	0.67	50.5
29	WHS11	FD	MCR	138.8	207.1	0.67	51.5
30	WKM2	FD	MCR-FCR	142.7	204.9	0.70	51.0
31	SMB9	FD	MCR-FCR	115.4	174.5	0.66	50.7
32	SMB14	FD	CCR-MCR	181.6	198.2	0.92	51.0

FABRIC PRESERVING AND FABRIC DESTROYING DOLOMITIZATION

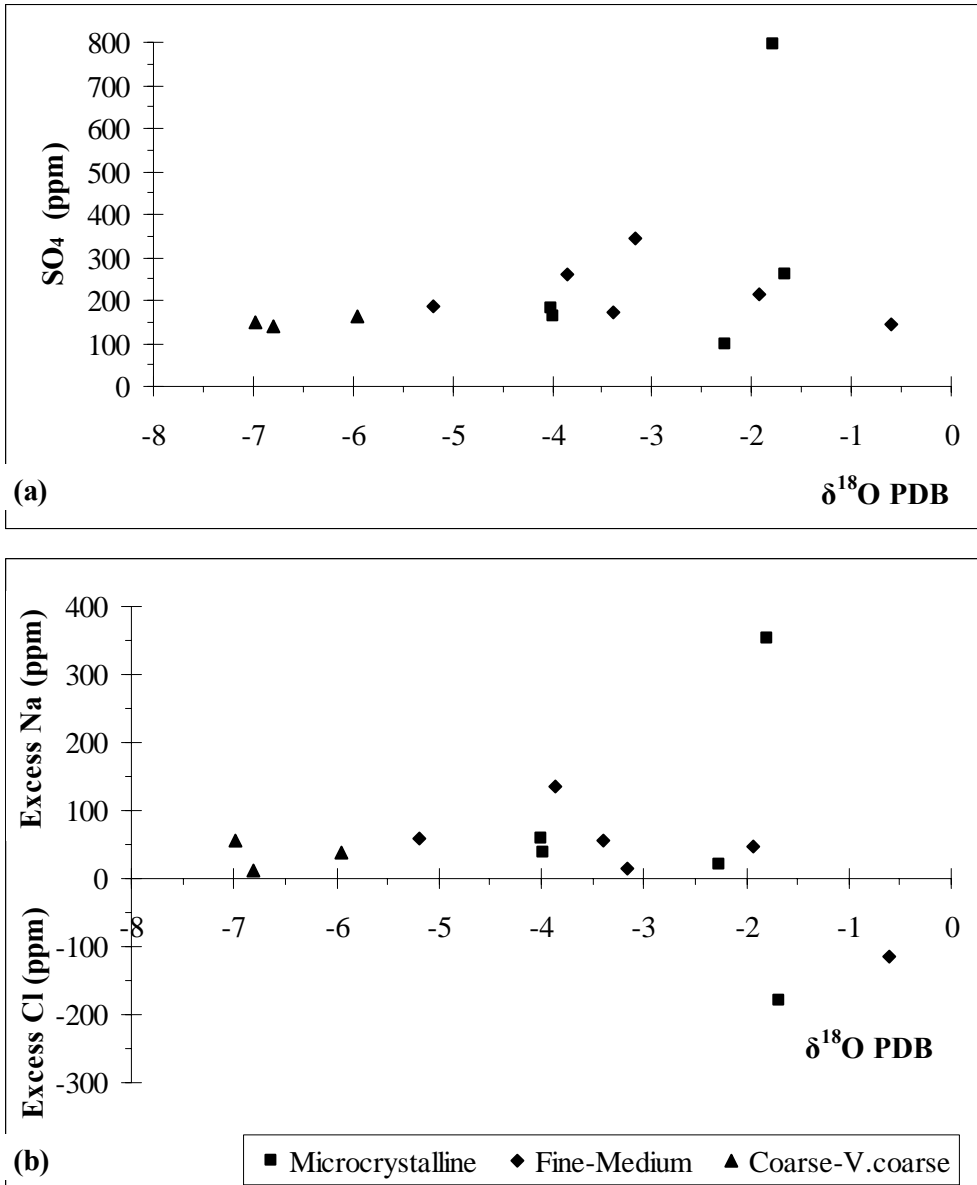


Figure 10. Relationship between crystal size and SO₄, excess Na and Cl, and oxygen isotopes concentrations in dolomites.

ALHAM JASSIM AL-LANGAWI

Table 2. Trace-elements concentration and stoichiometry in the dolomite samples. Cl and SO₄ were analyzed by ion chromatography, all other elements by atomic absorption.

Sample No.	Stratigraphic Position (m)	CaCO ₃ Mole%	Al	Si	Sr	Fe	Mn	Na	Cl	SO ₄
(ppm)										
Ruus Al Jibal Group (Locations 1-8).										
WBG2	203	51.87	1370	1693	130	945	133	114	118	136
WBG3	197	51.6	1205	1636	155	871	77	161	218	100
WBH1	175	50.51	462	702	181	579	83	136	109	91
WBH3	171	50.08	0	14	61	264	66	63	268	118
WBH6	160	50.75	1149	1508	94	670	65	98	330	260
WBB5	81	50.1	172	234	133	511	69	150	142	184
WBB6	78	50.19	235	337	156	489	78	150	155	145
WBB9	72	50.72	257	405	156	387	32	64	194	211
WBB14	55	50.66	1800	2304	172	1131	70	358	240	630
WBB17	47	50.02	621	1018	450	459	33	182	85	350
Ruus Al Jibal Group (Location 9)										
BIH46	298	51.34	10	0		450	54	100	76	0
BIH45	292	51.08	43	73		402	56	139	93	88
BIH37	270	50.21	17	353		620	76	262	125	251
BIH33	258	53.74	389	231		548	73	149	146	172
BIH29	206	53.78	19	156		364	51	164	163	183
BIH10	41	53.52	109	234		478	54	175	115	100
BIH6	24	51.71	85	0		489	76	132	179	272
Hagil and Bih Formations From Wadi Hagil										
HAGIL1	67	53.48	169	415		657	39	155	101	0
HAGIL2	65	51.51	165	56		479	33	100	126	0
HAGIL3	62	52.06	95	631		397	31	192	107	0
HAGIL8	42	52.72	170	677		459	45	210	123	150
HAGIL16	25	50.28	34	260		265	55	87	125	0
HAGIL19	18	51.47	130	508		531	63	60	160	153
HAGIL22	10	52.72	109	234		383	67	77	136	100
The Akhdar Group (Wadi Bani Kharus and Wadi Hajir)										
WKM7	382	51.2	72	82	25	499	55	150	300	180
WKM2	218	51.01	103	119	56	194	10	206	136	236
WHS19	206	52.65	76	20	70	365	99	82	317	142
KHARUS18	137	50.98	155	488		388	87	100	111	0
KHARUS17	135	49.81	350	535		489	115	128	176	345
WHS18	134	50.32	0	59	146	147	76	222	258	171
WHS15	116	50.53	10	109	131	156	39	176	242	136
KHARUS13	114	51.8	145	432		497	104	132	145	163
KHARUS4	95	51.78	247	521		448	116	186	137	284
WHS11	85	51.54	0	50	117	88	30	276	345	109
WHS9	65	50.47	0	48	109	119	158	171	379	142
The Saiq Formation (Wadi Bani Harras)										
HARRAS2	160	49.25	124	598		455	48	102	102	0

FABRIC PRESERVING AND FABRIC DESTROYING DOLOMITIZATION

HARRAS4	155	50.99	65	1292		448	47	86	112	0
HARRAS5	151	49.15	23	1093		624	66	87	194	158
HARRAS6	117	49.38	0	339		328	54	131	207	0
HARRAS7	85	52.48	204	599		477	56	42	99	0
Sumeini Group-Maqam Formation Member B (Jebel Sumeini)										
SMB2	53	51.26	307	294	69	181	21			
SMB5	41	50.61	202	171	68	183	42	288	235	260
SMB9	27	50.69	193	118	130	194	31	222	265	250
SMB14	1	50.95	100	173	95	259	100	250	300	150

4.3 Stable isotopes.

Oxygen and carbon isotope analysis was carried out on samples with a range of textural and compositional variations from different locations throughout the Oman Mountains. Table 3 lists all the isotopic results from the Permian-Triassic dolomites of the various formations. Plotting $\delta^{18}\text{O}$ against $\delta^{13}\text{C}$ for all the samples (Figure 11) revealed that there are two distinct areas which can be differentiated and which relate to crystal size. The rocks displaying microcrystalline, fine and medium crystal sizes have nearly constant $\delta^{18}\text{O}$ and $\delta^{13}\text{C}$ values which are different from those of the coarse to very coarse crystal sizes. Figure 11 also shows that dolomite samples which are composed of coarse to very coarse crystals are depleted in $\delta^{18}\text{O}$ compared to rocks which are composed of finer sizes.

Table 3 and Figure 12, show that $\delta^{13}\text{C}$ values are higher in rocks of Permian age than those of Triassic age. A limestone sample from the Milaha Formation (WBM6) was tested for oxygen and carbon isotopes (Table 3). The isotopic values do not plot within any of the two areas which were differentiated according to crystal size (Figure 11a), but show a similar $\delta^{13}\text{C}$ to the Triassic dolomites (Figure 11b). All the coarse and very coarse dolomites and baroque dolomite crystals plot together in a relatively small field ranging between -5.954 to -8.470 $\delta^{18}\text{O}$ ‰ PDB and $+1.619$ to $+3.296$ $\delta^{13}\text{C}$ ‰ PDB. The microcrystalline to medium dolomite crystals plot in a wide field, scattered between -5.184 to $+0.095$ $\delta^{18}\text{O}$ ‰ PDB and -0.707 to $+5.848$ $\delta^{13}\text{C}$ ‰ PDB (Figure 12). Figure 12 suggests that microcrystalline to medium crystalline dolomite samples in this study could have developed due to replacement of host rocks in the shallow burial environments by modified seawater of a formation temperature of $\leq 60^\circ\text{C}$, and dolomitized early by normal marine waters. On the other hand, the coarse and very coarse crystalline dolomites and baroque dolomites may have developed under shallow burial conditions marked by increase in temperature. None of the Permian and Triassic dolomites falls within the composition interpreted as of mixed-water origin by Choquette and Steinen (1980) and sabkha origin presented by Perkins *et al* (1994) (Figure 12). Few microcrystalline and fine-medium crystalline samples fall within the field of mixed-water dolomites presented by Dunham and Olson (1980) (Figure 10).

4.4 Ion chromatography.

The ion chromatography technique of Staudt *et al.* (1993) apparently provides a way of differentiating environments of dolomitization. Plotting the results gained for Cl, SO_4 and Na against the graphs presented by Staudt *et al.* (1993) indicated some contradictions (Figures 13 and 14).

Table 3. Showing the distribution of oxygen and carbon isotopes within the Ruus Al Jibal and Akhdar Groups, Sumeini Group-Maqam Formation Member B, and Milaha Formation. FP=Fabric-Preserving Dolomitization, FD=Fabric-Destroying Dolomitization, Ruus al Jibal Group: (WBB, WBH, WBG, BIH, HAGIL), Milaha Formation:(WBM), Akhdar Group: Saiq Fm.(WHS, KHARUS, HARRAS), Mahil Fm. (WKM), Sumeini Group; Maqam Fm. Member B (SMB).

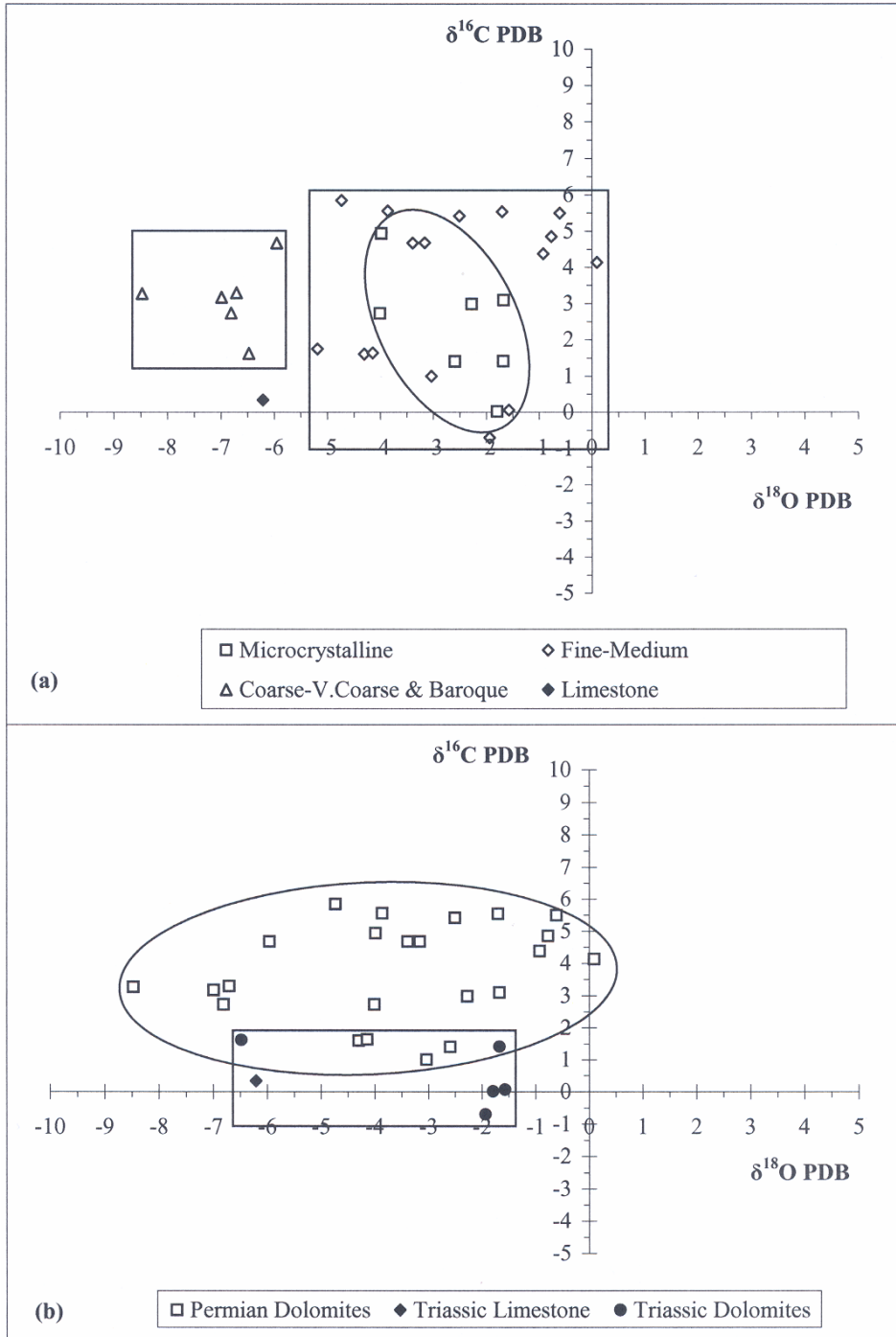


Figure 11. Distribution of oxygen and carbon isotopes within Permian-Triassic rocks from Oman Mountains: (a) according to crystal size, (b) according to age.

FABRIC PRESERVING AND FABRIC DESTROYING DOLOMITIZATION

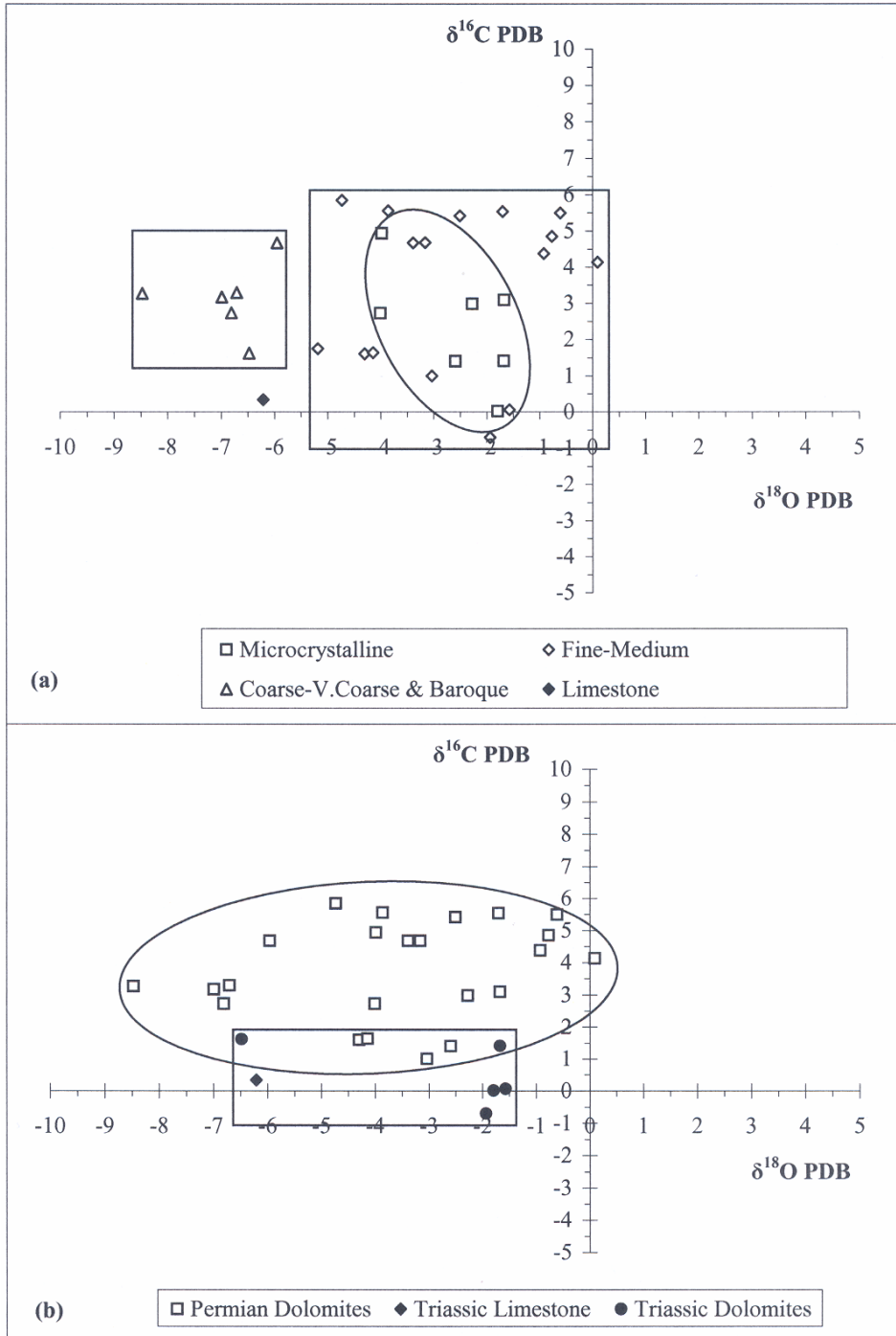


Figure 12. Correlating the isotopic data of the Oman Mountain dolomites with others inferred dolomitizing mechanisms. (PS)= Samples from the present study.

ALHAM JASSIM AL-LANGAWI

Table 3. Showing the distribution of oxygen and carbon isotopes within the Ruus Al Jibal and Akhdar Groups, Sumeini Group-Maqam Formation Member B, and Milaha Formation. FP=Fabric-Preserving Dolomitization, FD=Fabric-Destroying Dolomitization, Ruus al Jibal Group: (WBB, WBH, WBG, BIH, HAGIL), Milaha Formation: (WBM), Akhdar Group: Saiq Fm. (WHS, KHARUS, HARRAS), Mahil Fm. (WKM), Sumeini Group; Maqam Fm. Member B (SMB).

No.	Sample No.	Age	Texture FP/FD	Crystal Size and/or Rock Type	Oxygen PDB	Carbon PDB
1	WBB5	Permian	FD	Medium Crystalline	-5.184	1.746
2	WBB8-1	Permian	FP	Microcrystalline	-2.589	1.404
3	WBB8-2	Permian	FP	Intraform.Breccia (Fine-Medium)	-3.036	0.996
4	WBH6	Permian	FP	Microcrystalline	-1.671	3.091
5	WBG3	Permian	FP	Stromatolitic	-2.271	2.979
6	WBM6	Triassic	FP	Grainstone (LMS)	-6.209	0.335
7	BIH29-1	Permian	FP	Microcrystalline	-4.004	2.723
8	BIH29-2	Permian	FP	Baroque Cement	-6.807	2.730
9	BIH46	Permian	FD	Coarse Crystalline	-8.470	3.269
10	BIH50	Triassic	FP	Microcrystalline	-1.792	0.016
11	BIH54	Triassic	FD	Fine Crystalline	-1.934	-0.707
12	HAGIL16	Permian	FD	Medium Crystalline	-4.300	1.602
13	WHS7	Permian	FP	Grianstone (Fine-Medium)	-4.731	5.848
14	WHS9	Permian	FD	Fine Crystalline	-0.607	5.497
15	WHS17	Permian	FP	Oolitic Grainstone (Fine-Medium)	0.095	4.131
16	WHS18	Permian	FD	Fine-Medium Crystalline	-3.386	4.670
17	KHARUS1	Permian	FP	Bioclastic Grainstone (F-M)	-0.921	4.374
18	KHARUS13-1	Permian	FP	Coarse Sparry Cement	-5.954	4.671
19	KHARUS13-2	Permian	FP	Microcrystalline	-3.982	4.932
20	KHARUS17	Permian	FD	Fine-Medium Crystalline	-3.160	4.678
21	HARRAS7	Permian	FD	Fine-Medium Crystalline	-4.143	1.634
22	HARRAS8	Permian	FP	Packstone (Fine-Medium)	-0.767	4.850
23	WKM2	Triassic	FD	Fine-Medium Crystalline	-1.568	0.060
24	WKM6-1	Triassic	FP	Baroque Cement	-6.476	1.619
25	WKM6-2	Triassic	FP	Microcrystalline	-1.675	1.407
26	SMB5	Permian	FD	Fine Crystalline	-3.858	5.555
27	SMB10-1	Permian	FD	Medium Crystalline	-2.503	5.415
28	SMB10-2	Permian	FD	Fine Crystalline	-1.699	5.537
29	SMB10-3	Permian	FD	Coarse-V.Coarse Cement	-6.705	3.296
30	SMB14	Permian	FD	Medium-Coarse Crystalline	-6.987	3.168

While most of the values plot within the overlap field (Figure 13), but when plotting Na against Cl, analyses fall within the seawater/ mixing zone field (Figure 14). Baroque dolomite samples were also analyzed and they plot within the overlap and seawater/mixing zones of Figures 13 and 14.

FABRIC PRESERVING AND FABRIC DESTROYING DOLOMITIZATION

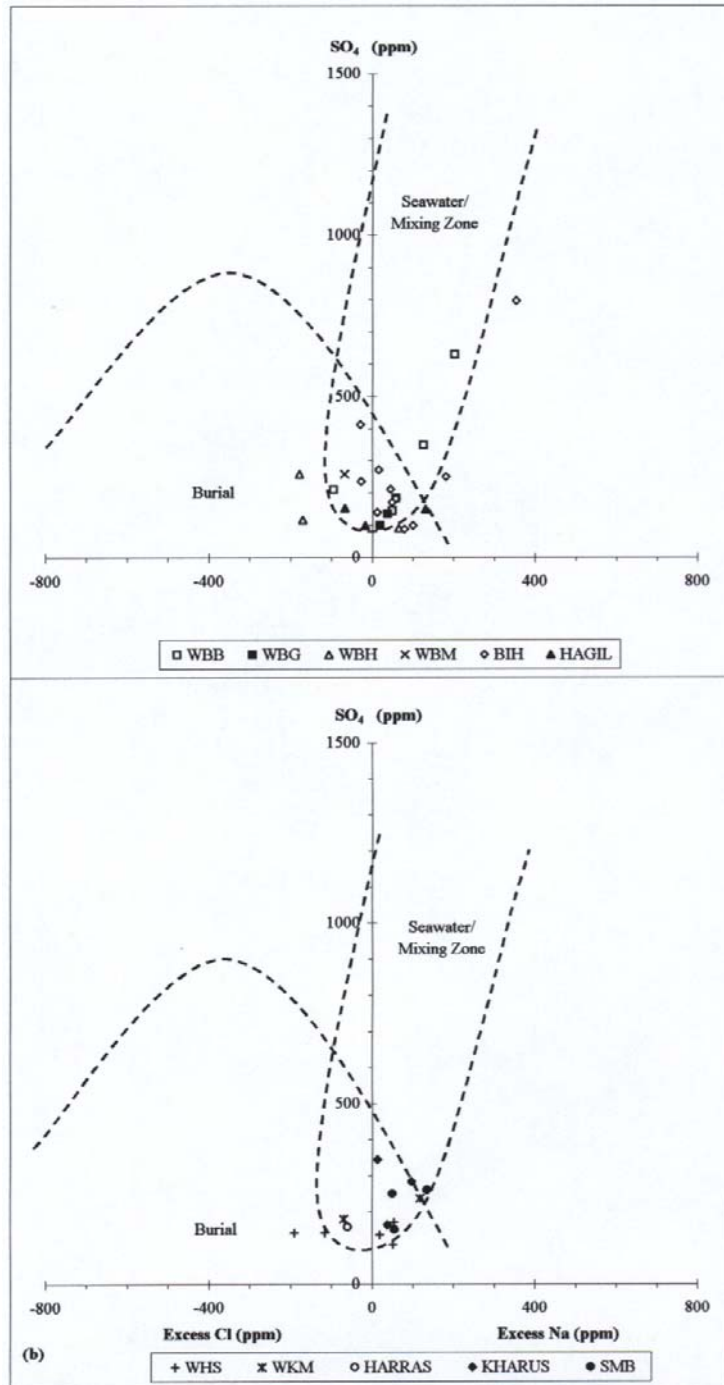


Figure 13. Environment of dolomitization for Oman Mountains Dolomites according to Staudt *et al* (1993) plot of excess Na and Cl against SO₄ concentrations in ppm.

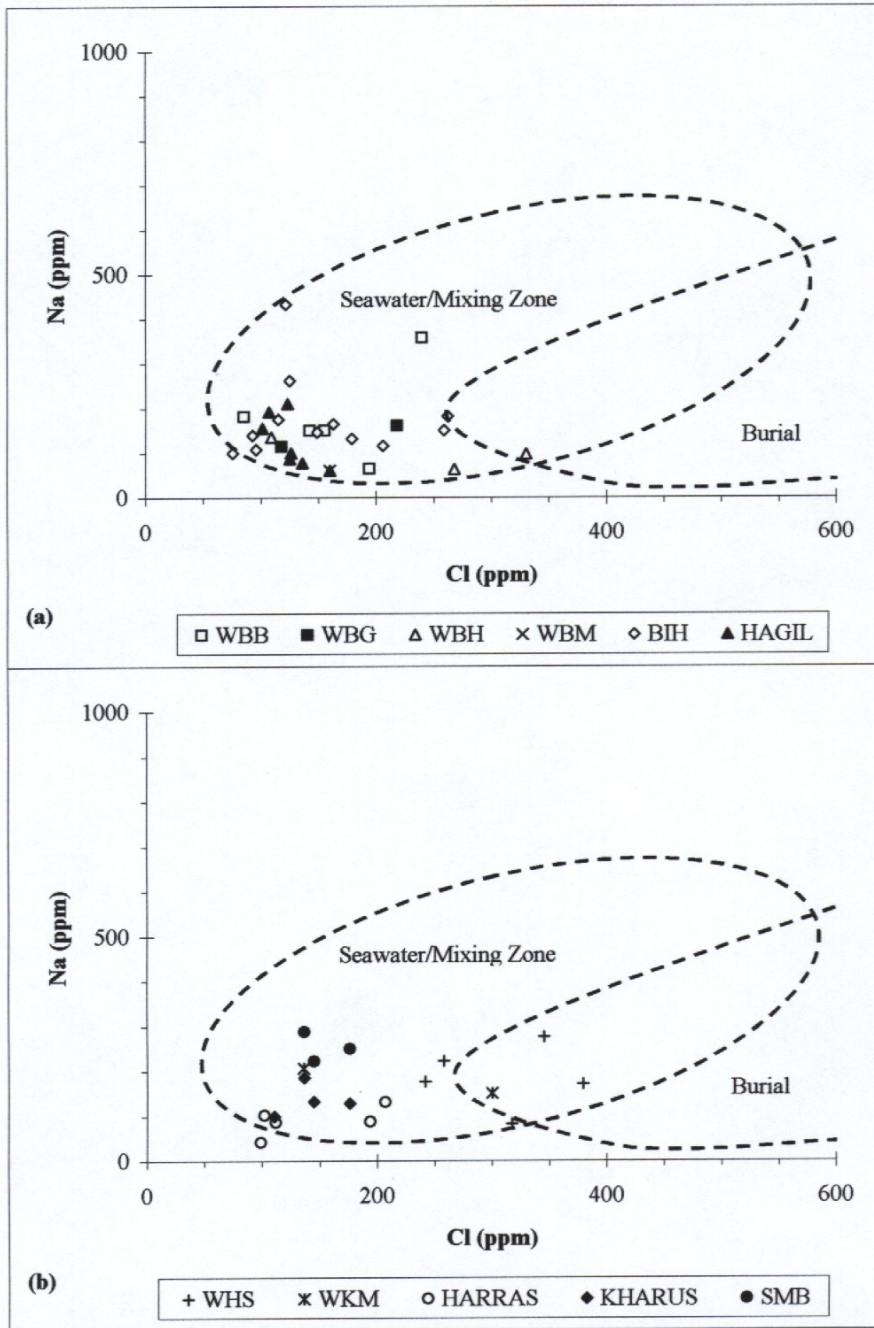


Figure 14. Environment of dolomitization for the Oman Mountain dolomites according to Staudt *et al* (1993) plot of Cl against Na concentrations in dolomites: (a) Samples from the Ruus Al Jibal Group and Milaha Formation. (b) Samples from the Akhdar Group and Sumeini Group-Maqam Formation Member B.

FABRIC PRESERVING AND FABRIC DESTROYING DOLOMITIZATION

Furthermore, some data points did not plot within any of the designated fields, and only four samples plot in the seawater/mixing zone fields of both figures and two samples in the overlap fields of both figures. However, these figures clearly suggest a non-evaporitic related dolomitization.

The above mentioned correlation between the isotopes and SO_4 concentrations indicates that the range produced by Staudt *et al.* (1993) for SO_4 in dolomites does not necessarily indicate a definite environment of dolomitization, especially in the overlap fields, which range between 40-570 ppm. As mentioned earlier, most of the Oman Mountain dolomite samples from all textural categories lie within this range, which made it difficult to interpret their environment of dolomitization, whether burial or seawater/ mixing zone dolomitization according to Staudt *et al.* (1993). Moreover, comparing the results on the relationship between oxygen isotopes, Cl and Na with the results from the method of Staudt *et al.* (1993) indicates that enrichment in Cl does not necessarily indicate burial conditions. These results also show that the microcrystalline dolomites from the Oman Mountains with oxygen isotope values close to equilibrium with near normal marine waters possess high Cl concentrations. Therefore, the isotope analysis was beneficial to verify the environment of deposition for the Oman Mountain dolomites while the method of Staudt *et al.* (1993) failed to elucidate or explain the relationship between the values gained and the environments of dolomitization.

5. Mechanisms of dolomitization and the possible source of dolomitizing fluids.

The dolomitization of a carbonate sediment composed of 100% high Mg-calcite using the connate water will produce ~ 30% dolomite (Tucker and Wright, 1990), assuming the existence of a reasonably high original porosity. Therefore, even if all the Mg from the allochems is totally consumed in producing the dolomites, there was insufficient Mg in the host rock to account for dolomitization. Consequently, this must be compensated by other Mg-sources, such as marine water, formation waters and migrating brines, in order to produce massive dolomite sequences. The extent of change will depend upon the initial porosity and permeability relationships of the host sediment/rock. The fact that nearly the entire thickness of the examined rock groups in this study was totally dolomitized indicates that these petrographical properties were very favourable. However, a viable mechanism must operate to affect the mass transfer of fluids required. To cause the pervasive dolomitization of a thick sequence a major requirement is the vast through-put of fluids needed. The envisaged system must satisfy the mass transfer requirement of Mg with time.

The perfect preservation of host rock structures and textures indicates very early dolomitization, probably prior to any early diagenetic alteration, and in a relatively short time interval, before the end of the Triassic. Fast nucleation will produce very fine crystals which preserve original allochem structure and host rock textures. The only fluid capable of such dolomitization and in a short time interval is warm seawater circulating in the shallow subsurface. The rocks that underwent fabric-destroying dolomitization, and especially those displaying coarse crystalline textures, reflect several stages of dissolution-reprecipitation and neomorphism of dolomite in the shallow subsurface by marine and/or mixed waters, as indicated by the isotopic values and trace elements.

The palaeogeography indicates that the Oman region was situated at the edge of the Arabian Craton, away from the recharge area in the west and thus affected by seawater supplied from the vast Tethys Ocean to the east with the potential for dolomitization (Figure 15). The geothermal gradient increased in Early to Late Permian when the rifting of the Arabian Craton started (Blendinger *et al.* 1990; Robertson and Searle, 1990). Rifting and sea floor spreading during the Permian and Triassic increased the circulation of hot subsurface marine waters towards the edge of the Arabian platform (Oman Mountains) (Glennie *et al.*, 1974; Bechennec *et al.*, 1990; Robertson and Searle, 1990), allowing greater influx of warm waters capable of dolomitization in short time interval (Figure 15). Dolomitization may have occurred during the times when sea level was at its lowest levels which led to the migrating of the mixing zones toward the east (seaward).

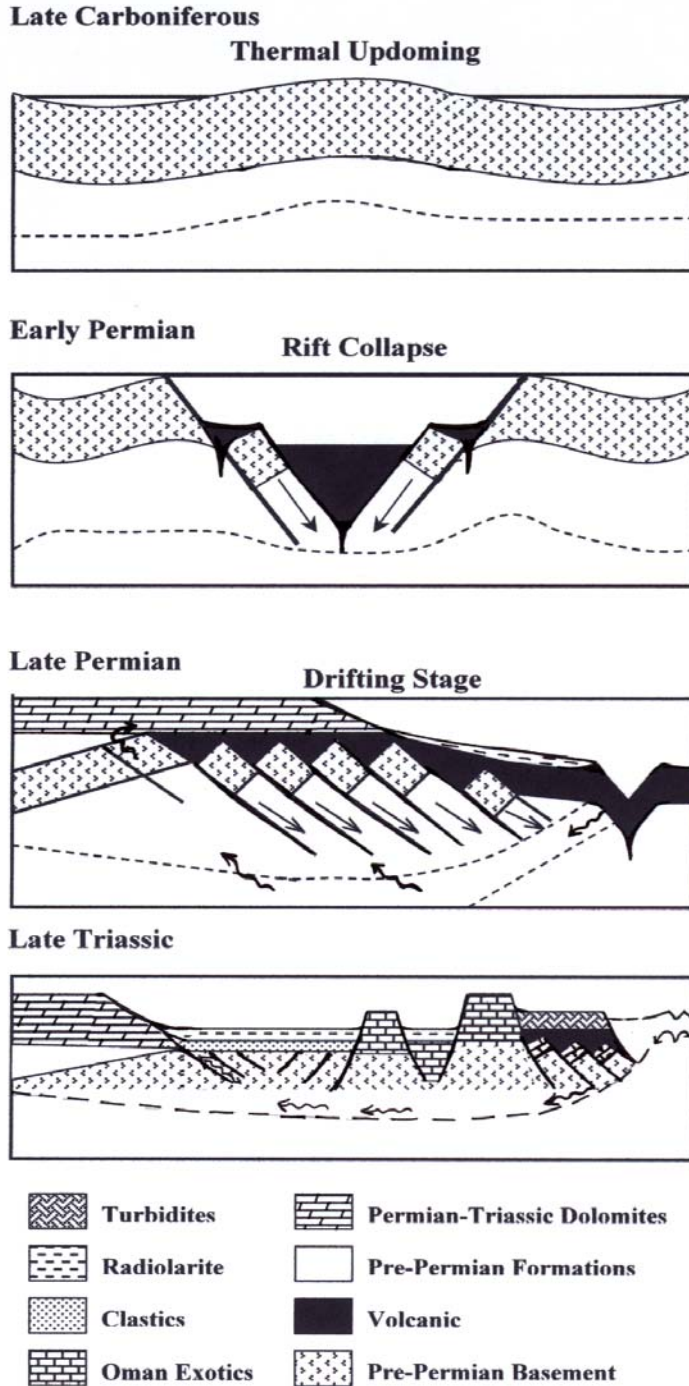


Figure 15. Permian and Triassic sea floor spreading and its effect on the geothermal gradient and movement of warm subsurface waters. Modified after Blendinger *et al.* (1990).

FABRIC PRESERVING AND FABRIC DESTROYING DOLOMITIZATION

The mixing between marine fluids from the east and evaporitic brines from the vast evaporitic-shelf on the Arabian Platform during Permian and Triassic times would also have been a possible source of fluids for dolomitization.

Because the Permian and Triassic dolomites from the Oman Mountains show a wide range of textural preservations and chemical variations it is hard to attribute dolomitization to one single process. All the results indicate the interplay of different dolomitizing conditions through time, mainly early dolomitization by normal seawater and modified marine waters by increased temperature, and relatively warm marine water conditions in the shallow subsurface.

6. Conclusion

The Permian and Triassic carbonates from the Oman Mountains display a great variety of textures embracing most, if not all, sedimentological dolomite variations known in the literature. They show a range from fabric-preservation to complete obliteration of host limestones textures. There is also fracture cementation as well as replacement of whole rocks by baroque dolomite. This petrographic study presented evidence on the systematic distribution of carbonate types between the north and the south in Oman Mountains. The samples from the Musandam peninsula are mainly rocks deposited in a supratidal and lagoonal environments, whereas most of the samples from the southern parts of Oman Mountains are rocks deposited in high energy environments such as shoals, reefs and back reefs.

The most important factor controlling the type of dolomite preservation (fabric-preserving or fabric-destroying) is the diagenetic stages that host rocks underwent prior to dolomitization. Early mimetic replacement by dolomite, prior to any exposure to meteoric waters and/or mixed waters, is important in producing dolomites which retain host rock textures. The combination of petrographic features and geochemistry in these dolomites suggests two main dolomitization stages. The first started soon after deposition in a marine setting either after or prior to cementation by high Mg-calcite and/or aragonite. This stage shows the following features: (i) Mimetic replacement of the micritic parts of allochems, micrite envelopes and matrix by cloudy nonplanar microcrystalline dolomites, (ii) Replacement of the bioclasts by fine cloudy nonplanar dolomites, (iii) Mimetic replacement of the first stage cement (high Mg-calcite or aragonite), where present, by cloudy dolomite crystals, and (iv) Development of clear-rhombic isopachous dolomite cement on the outer surface of allochems.

The second stage dolomite is a cement which shows competitive growth in to cavities. Variations in the composition of this cement are reflected in the zoned patterns seen under cathodoluminescence, and confirmed by microprobe analyses obtained from sequential points in single crystals.

The poor ordering, slightly Ca-rich composition to near stoichiometry, textural preservation features, trace element composition, especially high Al, Si and Na, and enrichment to slight depletion in ^{18}O values are features compatible with other dolomites inferred to have developed early under normal and near normal marine fluids. On the other hand, well ordered rock-forming dolomites, near to stoichiometric compositions, with a crystalline texture, low Na, Fe and depleted ^{18}O values, are features compatible with dolomites inferred to have formed under oxidising mixed and marine waters in the shallow subsurface under temperatures not higher than 60°C . Moreover, stable isotopes in various types of dolomites suggest two main dolomitizing fluids. The isotopic data are compatible with seawater and mixed water dolomitization. The marine fluids could be of near-normal seawater composition and/or slightly modified marine fluids by heat and evaporation.

Therefore, in the absence of any evidence of hypersaline brines and the relative sparsity of evidence for dolomitization during burial, the Permian and Triassic carbonates of the Oman Mountains must have been dolomitized early in diagenesis by marine-derived fluids perhaps mixed with varying amounts of meteoric water. The only fluid capable of early dolomitization, which is marked by host-rock/sediment preservation in a short time interval, is warm seawater from the vast Tethys Ocean. Seafloor spreading which was initiated during the Late Permian and Triassic was an important factor in elevating the geothermal gradient in the shallow subsurface during dolomite development. Mixing zone dolomitization may have developed during several sea level

lowstands during the Permian and Triassic, when shifting of the dolomitization environments to the east occurred.

7. References

- ADAMS, A.E., MACKENZIE, W.S., and GUILFORD, C. 1984. *Atlas of sedimentary rocks under the microscope*. Longman Group Limited.
- BECHENNEC, F., LE METOUR, J., RABU, D., BOURDILLON-DE-GRISSAC, CH., DE WEVER, P., BEURRIER, M. and VILLEY, M. 1990. The Hawasina Nappes: Stratigraphy, palaeogeography and structural evolution of a fragment of the south-Tethyan passive continental margin. In *The Geology and Tectonics of the Oman Region*. eds A.H. F. Robertson, M.P. Searle and A.C. Ries, Geological Society, London, Special Publication, No.49, pp. 213-223.
- BLENDINGER, W., VAN VLIET, A., and HUGHES CLARKE, M.W. 1990. Updoming, rifting and continental margin development during the Late Palaeozoic in northern Oman. In *The Geology and Tectonics of the Oman Region*. eds A.H.F. Robertson, M.P. Searle and A.C. Ries, Geological Society, London, Special Publication, No.49, pp. 27-37.
- BULLEN, S.B. and SIBLEY, D.F. 1984. Dolomite selectivity and mimic replacement. *Geology*, **12**: 655-658.
- CHOQUETTE, P.W. and STEINEN, R.P. 1980. Mississippian non-supratidal dolomite, Ste.Genevieve limestone, Illinois Basin: evidence for mixed-water dolomitization. In *Concepts and Models of Dolomitization*. eds, D.H. Zenger, J.B. Dunham, and R.L. Ethington. Society of Economic Palaeontologists and Mineralogists, Special Publication, No.28, pp.163-196.
- DELGADO, F. 1977. Primary textures in dolostones and recrystallized limestone: A technique for their microscopic study. *Journal of Sedimentary Petrology*, **47**:1339-1341.
- DUNHAM, J.B. and OLSON, E.R. 1980. Shallow subsurface dolomitization of subtidally deposited carbonate sediments in the Hanson Creek Formation (Ordovician-Silurian) of Central Nevada. In *Concepts and Models of Dolomitization*. eds D.H. Zenger and J.B. Dunham. Society of Economic Palaeontologists and Mineralogists, Special Publication, No. 28, pp.139-162.
- GLENNIE, K.W., BOEUF, M.G. A., HUCHES CLARKE, M.W., MOODY-STUART, M., PILAAR, W.F.H., and RIENHARDT, B.M. 1974. Geology of the Oman Mountains. *Verhandelingen Van Hert Koninklijk Nederlands geologisch mijnbouwkundig Genootschap*, **31**.
- MILLER, J.K. and FOLK, R.L. 1994. Petrographic, geochemical and structural constraints on the timing and distribution of post lithification dolomite in the Rhaetian Portoro ('Calcar Nero') of the Portovenere Area, La Spezia, Italy. In *Dolomites: A Volume in Honour of Dolomieu*. eds B.H. Purser, M.E. Tucker, and D.H. Zenger. *International Association of Sedimentologists*, Special Publication, No.21, pp.187-202.
- MURRAY, R.C. and LUCIA, F.J. 1967. Cause and control of dolomite distribution b rock selectivity. *Geologic Society of America Bulletin*, **78**: 21-35.
- MUTTI, M. and SIMO, J.A. 1994. Distribution, petrography and geochemistry of early dolomite in cyclic shelf facies, Yates Formation (Guadalupian), Capitan Reef Complex, USA. In *Dolomites: A Volume in Honour of Dolomieu*. eds B.H. Purser, M.E. Tucker, and D.H. Zenger. *International Association of Sedimentologists*, Special Publication, No.21, pp. 91-109.
- PERKINS, R.D., DWYER, G.S., ROSOFF, D.B., FULLER, J., BAKER, P.A., and LLOYD, R.M., 1994. Salina sedimentation and diagenesis: West Caicos Island, British West Indies. In *Dolomites: A Volume in Honour of Dolomieu*. eds B.H. Purser, M.E. Tucker, and D.H. Zenger. *International Association of Sedimentologists*, Special Publication, No.21, pp. 37-54.
- PURSER, B.H., TUCKER, M.E., and ZENGER, D.H., 1994a. Problems, progress and future research concerning dolomites and dolomitization. In *Dolomites: A Volume in Honour of Dolomieu*. eds PURSER B.H., TUCKER M.E., and ZENGER D.H. *International Association of Sedimentologists, Special Publication*, No.21, pp. 3-20.

FABRIC PRESERVING AND FABRIC DESTROYING DOLOMITIZATION

- PURSER, B.H., BROWN, A., and ASSAOUI, D.M. 1994b. Nature, origin and evolution of porosity in dolomites. In *Dolomites: A Volume in Honour of Dolomieu*. eds PURSER, B.H., TUCKER, M.E., and ZENGER, D.H. *International Association of Sedimentologists*, Special Publication, No.21, pp. 283-308.
- ROBERTSON, A.H.F. and SEARLE, M.P. 1990. The northern Oman Tethyan continental margin: stratigraphy, structure, concepts and controversies. In *The geology and tectonics of the Oman region*. eds ROBERTSON, A.H.F., SEARLE, M.P., and RIES, A.C. *Geological Society*, London, Special Publication, No.49, pp. 3-25.
- SCHOLLE, P.A. 1978. A color illustrated guide to carbonate rock constituents, textures, cements and porosities. *American Association of Petroleum Geologists*, Memoir, No. 27.
- SIBLEY, D.F. 1980. Climatic control of dolomitization, Seroe Domi Formation (Pliocene), Bonaire, N.A. In *Concepts and Models of Dolomitization*. eds ZENGER, D.H., DUNHAM, J.B., and ETHINGTON, R.L. *Society of Economic Palaeontologists and Mineralogists*, Special Publication, No.28, pp. 247-258.
- SIBLEY, D.F. 1982. The origin of common dolomite fabrics. *Journal of Sedimentary Petrology*, **52**: 1987-1100.
- SIBLEY, D.F. 1990. Unstable to stable transformations during dolomitization. *Journal of Geology*, **98**: 247-258.
- SIBLEY, D.F. and GREGG, J.M. 1987. Classification of dolomite rock textures. *Journal of Sedimentary Petrology*, **57**(6): 967-975.
- STAUDT, W.J., OSWALD, E.J., and SCHOONEN, M.A.A. 1993. Determination of sodium, chloride and sulfate in dolomites: a new technique to constrain the composition of dolomitizing fluids. *Chemical Geology*, **107**: 97-109.
- TUCKER, M.E. and WRIGHT, P. 1990. *Carbonate Sedimentology*. Blackwell Scientific Publications. Oxford-London.
- ZENGER, D.H. 1979. Primary textures in dolostones and recrystallized limestones: a technique for their microscopic study. *Journal of Sedimentary Petrology*, **49**: 677-678.
-

Received 8 February 2006

Accepted 22 November 2006